

RESEARCH ARTICLE

A versatile cell-penetrating peptide-adaptor system for efficient delivery of molecular cargos to subcellular destinations

Verra M. Ngwa^{1‡a}, David S. Axford², Allison N. Healey^{3‡b}, Scott J. Nowak², Carol A. Chrestensen¹, Jonathan L. McMurry^{2*}

1 Department of Chemistry & Biochemistry, Kennesaw State University, Kennesaw, Georgia, United States of America, **2** Department of Molecular & Cellular Biology, Kennesaw State University, Kennesaw, Georgia, United States of America, **3** New Echota Biotechnology, Kennesaw, Georgia, United States of America

‡a Current address: Department of Cancer Biology, Vanderbilt University School of Medicine, Nashville, Tennessee, United States of America

‡b Current address: Department of Agriculture & Biomedical Engineering, Mississippi State University, Starkville, Mississippi, United States of America

* jmcmurr1@kennesaw.edu



OPEN ACCESS

Citation: Ngwa VM, Axford DS, Healey AN, Nowak SJ, Chrestensen CA, McMurry JL (2017) A versatile cell-penetrating peptide-adaptor system for efficient delivery of molecular cargos to subcellular destinations. *PLoS ONE* 12(5): e0178648. <https://doi.org/10.1371/journal.pone.0178648>

Editor: Maxim Antopolsky, Helsingin Yliopisto, FINLAND

Received: February 8, 2017

Accepted: May 16, 2017

Published: May 26, 2017

Copyright: ©2017 Ngwa et al. This is an open access article distributed under the terms of the [Creative Commons Attribution License](https://creativecommons.org/licenses/by/4.0/), which permits unrestricted use, distribution, and reproduction in any medium, provided the original author and source are credited.

Data Availability Statement: All relevant data are within the paper and its Supporting Information files.

Funding: This work was supported by National Institute on General Medical Sciences (<https://www.nigms.nih.gov>) grants GM120691 (to JLM), GM102826 (to SJN) and GM110634 (to CAC). VMN was supported by NIH R25 GM111565 and DSA received a Birla Carbon Summer Undergraduate Research Fellowship (KSU College

Abstract

Cell penetrating peptides have long held great potential for delivery of biomolecular cargos for research, therapeutic and diagnostic purposes. They allow rapid, relatively nontoxic passage of a wide variety of biomolecules through the plasma membranes of living cells. However, CPP-based research tools and therapeutics have been stymied by poor efficiency in release from endosomes and a great deal of effort has been made to solve this ‘endosomal escape problem.’ Previously, we showed that use of a reversible, noncovalent coupling between CPP and cargo using calmodulin and a calmodulin binding motif allowed efficient delivery of cargo proteins to the cytoplasm in baby hamster kidney and other mammalian cell lines. The present report demonstrates the efficacy of our CPP-adaptor scheme for efficient delivery of model cargos to the cytoplasm using a variety of CPPs and adaptors. Effective overcoming of the endosomal escape problem is further demonstrated by the delivery of cargo to the nucleus, endoplasmic reticulum and peroxisomes by addition of appropriate subcellular localization signals to the cargos. CPP-adaptors were also used to deliver cargo to myotubes, demonstrating the feasibility of the system as an alternative to transfection for the manipulation of hard-to-transfect cells.

Introduction

Cell-penetrating peptides (CPPs, also known as protein transduction domains, or PTDs) allow transport of biomolecular cargo into an array of eukaryotic cells. Discovered some decades ago, there has been a great deal of interest ever since, including development of an array of CPP moieties [1, 2] and strategies for linkage to cargo. Cargo can be virtually any biomolecule, ranging from large protein complexes [3] to small molecules to siRNA and other nucleic acids [4]. Their promise for therapeutics is high and more than 25 clinical trials are underway [5–7],

of Science & Mathematics, <http://csm.kennesaw.edu/>). New Echota Biotechnology provided support in the form of salary to ANH, but did not have any additional role in the study design, data collection and analysis, decision to publish, or preparation of the manuscript. The specific roles of these authors are articulated in the 'author contributions' section. The funders had no role in study design, data collection and analysis, decision to publish, or preparation of the manuscript.

Competing interests: I have read the journal's policy and the authors of this manuscript have the following competing interests: JLM and SJN have equity interest in New Echota Biotechnology, which has exclusive license to pending patents (US 2016/0355561 14/545,637 and PCT/US17/16189 62/290,629 on the CPP-adaptor technology and applications thereof. The other authors have no competing interests. This does not alter our adherence to PLOS ONE policies on sharing data and materials.

but progress has been lacking due to a number of specific challenges including cargo coupling strategies, lack of cell specificity and poor endosomal escape.

It has long been noted that high doses of CPP-cargo fusions are required to generate measurable quantities in the cytoplasm as perhaps less than 1% of delivered cargo reaches the cytoplasm [8], and the dawning realization is that the vast majority CPPs get trapped in endosomes and targeted for degradation rather than released into the cytoplasm. The mechanism of entry is unclear, though receptor-mediated endocytosis is the most likely general mechanism [9, 10] with heparin sulfate proteoglycans as CPP receptors [11]. Perhaps high affinities of CPPs for their receptors are the reason why entrapment occurs.

Endosomal escape (also referred to as 'endosomolysis') remains a significant barrier to the adoption of CPP therapies and other applications. Several strategies have been developed to address this shortcoming. Use of endosomally cleavable peptides had a salutary effect on treatment of tumors in mice with a CPP-delivered toxin [12]. Other attempts include thiol [13] and photocleavable linkages [14]. Our prior report [15] was the first to use a specific, high-affinity, reversible noncovalent linkage to mediate cargo attachment to CPP moiety, thus overcoming the endosomal escape problem in a novel way.

Our prototype CPP-adaptor, TAT-CaM, consists of the CPP moiety of TAT [16] fused to human calmodulin (CaM). Calmodulin is a calcium biosensor that folds into a dumbbell-shaped conformation in the presence of Ca^{2+} [17–20], closing around a 17-residue calmodulin binding site (CBS) on target proteins. Binding of CaM to CBS motifs is around 1 nM in affinity in the presence of calcium but negligible in its absence [21]. Cargo proteins were expressed with a canonical CBS at the N-terminus. Cargos and CPP-adaptors bind spontaneously and rapidly in the presence of Ca^{2+} . However, most mammalian cells maintain a low resting concentration of cytoplasmic calcium, typically ~ 100nM, ~20,000x less than extracellular concentrations [22] and endocytosed Ca^{2+} is rapidly released from endosomes [23]. Thus, cargos are released within minutes of entry even though the CPP-adaptor remains entrapped in the endosome. Importantly, significant release from the endosome was achieved at 1 μM , 10-100-fold less covalently linked CPP-cargos [8].

Thus, our system presents a solution to the endosomal escape problem through a penetration-then-release mechanism. In the present study, we sought to assay the generalizability of our scheme by using other CPP moieties SAP and SAP(E) [24, 25] and alternative EF hand proteins CALML3 [26] and troponin [27] as adaptors. All constructs delivered their cargos rapidly and with high efficiency, achieving cytoplasmic distribution within 1 hour, likely much faster.

We also sought to adapt our CPP-adaptor/cargo complexes to deliver to subcellular destinations. CPP-mediated delivery of cargo to places other than the cytoplasm has long been a goal of developing therapeutics as there are many sites of action [28]. By addition of localization signals to cargo proteins, delivery to the nucleus, peroxisomes and endoplasmic reticulum was achieved.

Lastly, our method holds the prospect to become a high-efficiency alternative to transfection. By far the most common method to manipulate mammalian cells is transfection. While tremendous efforts have been made to improve transfection efficiencies, they remain disappointing and many cell types are resistant to transfection. In our previous report [15] we noted that all cells in the populations to which we had delivered cargo received it, i.e. there was 100% efficiency. Hypothesizing that whatever barriers transfection encounters, they are not germane to CPP-mediated delivery, our CPP-adaptors were successfully used to deliver cargo to myotubes, suggesting that our adaptor system may be a useful alternative to liposome-mediated transfection, capable of delivering cargo of choice to a differentiated tissue structure.

Materials and methods

Strains and cell lines

E. coli strains NovaBlue (EMD Millipore, USA) and BL21(DE3)pLysS (Thermo Fisher, USA) were used, respectively, to propagate plasmids and express proteins. BHK21 (#CCL-10) and C2C12 mouse myoblasts (#CRL-1772) cells were purchased from ATCC. BHK was cultured in Dulbecco's Modified Eagles' Medium supplemented with 10% fetal bovine serum, 4 mM glutamine, and 4.5 g/L glucose. Myoblasts were cultured as described [29].

Overexpression, purification and labeling

Plasmids encoding TAT-CaM and CBS-myoglobin have been previously described [16]. Genes encoding SAP-CaM, SAP(E)-CaM, TAT-Troponin (TAT-Tropo), TAT-calmodulin-like protein 3 (TAT-CALML3) were synthesized and cloned (Genewiz, South Plainfield, NJ) into *NdeI* and *BamHI* sites in pET19b (EMD Millipore, USA). Troponin inhibitory peptide-myoglobin (TIP-myo)[26] and CBS-myoglobins with C-terminal consensus subcellular localization signals for the nucleus (NLS), endoplasmic reticulum (KDEL) and peroxisomes (SKL) and CBS- α -tubulin were synthesized and cloned into *BamHI* and *HindIII* sites on pCAL-N-FLAG (Agilent Technologies, CA, USA), which encodes a calmodulin binding peptide and FLAG epitope N-terminal to the *BamHI* site. All synthetic genes were codon-optimized for expression in *E. coli*. Plasmids are listed in Table 1.

Proteins were expressed essentially as described [30]. Briefly, plasmids were transformed into BL21(DE3)pLysS. Overnight cultures were subcultured into 1L Luria-Bertani Broth and grown with vigorous shaking at 30°C. At OD₆₀₀ ~0.4 cells were induced with 0.2 mM IPTG and growth continued for four hours. Cells were harvested and frozen at -80°C.

Purification was also performed essentially as described [15], with CPP constructs purified via immobilized metal affinity chromatography and CBS-cargo constructs purified using a Calmodulin Sepharose column (GE Life Sciences, Pittsburgh, PA, USA). Proteins were exchanged into 10 mM HEPES, 150 mM NaCl, 10% glycerol for biotinylation or fluorescence labeling, both of which were accomplished by amine crosslinking. For biotinylation of CPP constructs used in optical biosensing experiments, NHS-LC-LC biotin was crosslinked per the manufacturer's protocol (ThermoFisher, USA). For confocal microscopy experiments,

Table 1. Plasmids used in this study.

Identifier	Descriptor	Parent Vector	Description	Relevant GenBank Accession #s
pJM996	TAT-CaM	pET19b	N-His-TAT-CaM	NP_001734.1
pJM1000	TAT-CaM 2.0	pET19b	N-His-TAT-CaM without GS C-terminal to TAT	NP_001734.1
pJM995	CBS-myo	pCAL-N-FLAG	N-CBS-myoglobin	AAA59595.1
pJM1002	SAP-CaM	pET19b	N-His-SAP-CaM	NP_001734.1
pJM1003	SAP(E)-CaM	pET19b	N-His-SAP(E)-CaM	NP_001734.1
pJM1001	TAT-CALML3	pET19b	N-His-TAT-calmodulin like protein 3	NP_005176.1
pJM1020	TAT-troponin	pET19b	N-His-TAT-troponin	NP_003270.1
pJM1021	TIP-myo	pET19b	N-His-CBS-troponin inhibitory peptide-myoglobin	AAA59595.1
pJM985	Myo-NLS	pCAL-N-FLAG	N-CBS-myoglobin-NLS	AAA59595.1
pJM1022	Myo-KDEL	pCAL-N-FLAG	N-CBS-myoglobin-KDEL	AAA59595.1
pJM987	Myo-SKL	pCAL-N-FLAG	N-CBS-myoglobin-SKL	AAA59595.1
pJM1023	CBS-tubulin	pCAL-N-FLAG	N-CBS-tubulin α 1A (mouse)	NP_035783.1

Plasmids used in this study. Accession numbers are for the naturally occurring gene from which codon-optimized sequences were generated.

<https://doi.org/10.1371/journal.pone.0178648.t001>

DyLight 550 was similarly crosslinked to cargo proteins or TAT-CaM and dye removal columns were used to remove unreacted dye (ThermoFisher). All proteins were exchanged into binding buffer (10 mM Tris, 150 mM NaCl, 10% glycerol, 1 mM CaCl₂ pH 7.4) by passage over a gel filtration column prior to analysis.

Optical biosensing

All biolayer interferometry measurements were carried out on a FortéBio (Menlo Park, CA) Octet QK biosensor with streptavidin sensors at 25°C on 96-well opaque plates. All volumes were 200 µl. Biotinylated CPP constructs were loaded for 300s after which sensors were moved to binding buffer only and a baseline was established. Association and dissociation phases were 300s each. Raw data were reference subtracted against the signal from a ligand-loaded sensor against buffer only and were then fit using a global one-state association-then-dissociation model with GraphPad Prism 5.03, from which kinetic and affinity constants were determined. Nonspecific binding was measured with respect to the response of 1 µM analyte protein against a sensor without ligand and was found to be negligible in all cases. Observation of rapid dissociation in the absence of calcium was accomplished by movement of the sensors into wells containing binding buffer with 10 mM EDTA and measuring nm shift for 300 s.

Cell penetration assays

1 µM each of TAT-CaM and DyLight 550-labelled cargo protein in buffer containing 1 mM CaCl₂ were added to subconfluent BHK21 cells and incubated for 1 hour, after which cells were washed three times in phosphate buffered saline with 1 mM CaCl₂. The cytoplasm was labeled by treatment with CytoTracker 488 Dye (Molecular Probes, USA). Cells were also labelled with NucBlue Live (Thermo Fisher, USA) and transferred to media containing 25 mM HEPES, pH 7.4 for imaging. Cells were immediately imaged on an inverted Zeiss LSM700 Confocal Microscope equipped with a 40x EC Plan-Neofluar objective (NA = 1.3). Pinholes for each fluorophore were set at 1.0 Airy Units (29 microns), and SP 490 and LP 615 filters were used to acquire the NucBlue (blue channel) and DyLight 550 (Red Channel) signals, respectively.

Z-stacks for both TAT-CaM-treated and untreated cells were set by using the NucBlue staining of the nucleus as a reference (typical Z-stacks ranged from 6.0–10.0 microns). Both treated (CPP-adaptor plus cargo) and untreated (cargo only) cells were imaged at identical gain settings, set at sub-saturation levels on cells treated with TAT-CaM in the red emission (DyLight 550 fluorescence). Both treated and untreated cells were imaged at an identical laser output level (2.0%, 555 nm laser), identical pixel dwell time of 3.15 microseconds, and 2x line averaging.

For analysis, images were rendered using the Orthogonal View in Zen Blue (Zeiss, Germany) software. Using the diameter of the nucleus as a landmark, the Z-plane chosen for analysis corresponded to approximately the mid-point depth of the nucleus. Finally, the DyLight 550 signal was analyzed separately and merged with NucBlue. For subcellular localization experiments, appropriate compartments (e.g., peroxisome, endoplasmic reticulum) were labeled with CellLight Peroxisome-GFP, BacMam 2.0 (Molecular Probes)[31], or ERTracker Dye (Molecular Probes), respectively according to the manufacturers' protocols.

Experiments to confirm TAT-CaM localization essentially as described above except that the TAT-CaM was labelled with DyLight 550, the cargo, CBS-myo was unlabelled and the complexes were added at equimolar ratios of 10 nM and 100 nM in separate experiments.

For delivery of protein cargo to myotubes, we first cultured C2C12 myoblasts on Matrigel-coated Ibidi plastic culture dishes (Ibidi, USA), under standard media conditions for growth

and differentiation [29]. Myotubes were differentiated for three days, and then protein cargos and labeling of myotubes, as well as imaging were performed as described above.

Results & discussion

A prior study demonstrated the utility of our CPP-adaptor strategy for delivery of molecular cargo to the interiors of cells with TAT-CaM and several different model cargos and several different cell lines [16]. All cargos were widely distributed in the cytoplasm and three different cell types were readily penetrated. The present results show extended utility of noncovalent coupling in the use of different CPP moieties, the differential fates of CPP-adaptors and cargos and effective distribution using subcellular localization signals.

The generalizability of the use of EF hand proteins and their cognate binding targets was open to question. We designed a second generation TAT-CaM, TAT-CaM, 2.0, to remove an extraneous pair of residues within the fusion tag that were the result of an unneeded restriction site engineered into the original synthetic gene; it is otherwise identical. We used calmodulin-like protein 3 (CALML3) and troponin as alternate EF hand proteins as well as SAP and SAP (E) as alternate CPP moieties of differing characteristics. As shown in Fig 1A–1E, CPP-adaptors bound their cargos with high affinities in the presence of calcium, as expected. The cargo protein was CBS-myo for all CPP-adaptors save TAT-Troponin, for which the cargo was troponin inhibitory peptide-myoglobin, TIP-myo.

Affinities ranged from 13–30 nM. k_{off} and K_D were indeterminate for TAT-CaM 2.0 and TAT-troponin binding to their cargos as anomalies in the early parts of the dissociation phases made determination of their very low off rates impossible; suffice it to say their k_{off} s are very low and the affinity of TAT-CaM 2.0 and TAT-troponin for their cargos is very high in the presence of calcium.

The identities of the cell-penetrating sequence and EF hand proteins did not significantly affect binding kinetics as SAP and SAP(E) were indistinguishable from TAT-CaM 2.0, which itself is indistinguishable from TAT-CaM [16]. Other adaptors using alternate EF hand proteins, TAT-CALL3 and TAT-troponin, bound their targets with high affinity. On rate constants for all constructs are on the order of $10^3 \text{ M}^{-1} \text{ s}^{-1}$ and off rate constants are $\sim 10^{-4} \text{ s}^{-1}$ or slower, in good agreement with our prior measurements for TAT-CaM and several model cargos [16] as well as wild-type calmodulin [22]. Kinetic parameters are shown in Table 2.

All CPP-CaM-cargo complexes exhibited very fast dissociation ($\sim 10^{-1} \text{ s}^{-1}$) when exposed to EDTA (Fig 1F), as expected and previously shown of calmodulin and its regulated proteins in upon the removal of calcium [15, 21, 32, 33]. Interestingly TAT-Tropo exhibited slower, but still rapid dissociation ($1.8 \times 10^{-2} \text{ s}^{-1}$). This may be due to the conformational shift of troponin C that accompanies Ca^{2+} dissociation being slow compared to calmodulin [26], though it may also represent some other difference in CPP-adaptor/cargo pair. However, regardless of particular CPP, adaptor or binding sequence, all CPP-adaptor/cargo pairs bound with high affinity in the presence of calcium and low affinity in its absence, demonstrating that our overall design of high-affinity, reversible cargo coupling is valid.

Cell penetration experiments likewise demonstrated effective delivery and cytoplasmic distribution of cargo proteins in BHK cells (Fig 2). In the presence of an equimolar (1 μM) concentration of the CPP-adaptor, all fluorescently labelled cargo proteins colocalized with cytoplasmic tracking dye. When CPP-adaptors were absent, fluorescence was negligible, which was underscored by its absence at the same cytoplasmic depth as evidenced by the orthogonal projections, i.e. the fluorescence present in the absence of CPP-adaptors is due to nonspecific adherence to the outside of the cell. Attempts to characterize the kinetics of penetration failed as there was no condition under which we could observe the cargo in which it

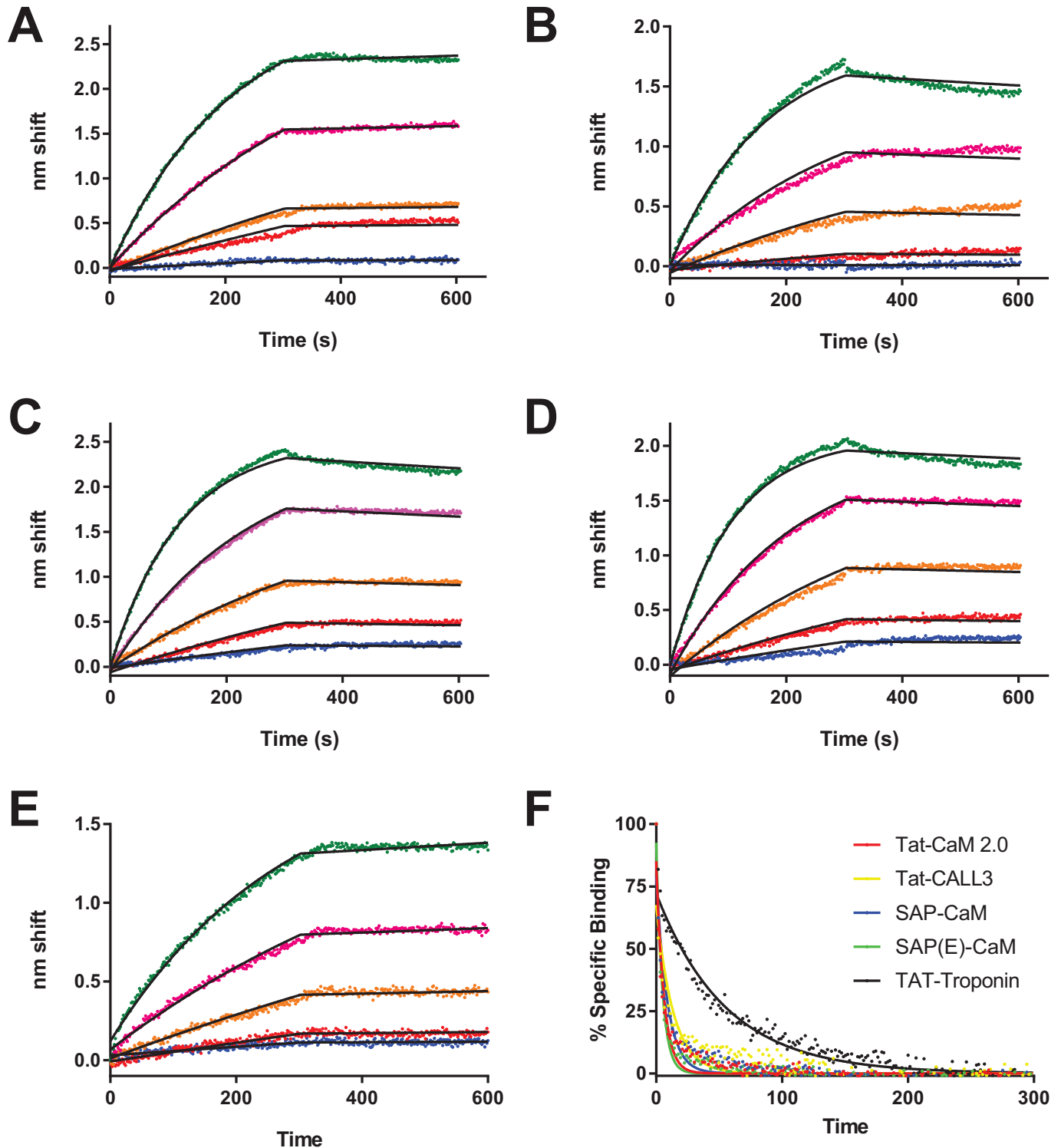


Fig 1. Biolayer interferometry analysis of CPP-adaptor-cargo binding. Association (0-300s) and dissociation (300-600s) phases are shown for A, TAT-CaM; B, TAT-CALL3; C, SAP-CaM; D, SAP(E)-CaM and E, TAT-Troponin binding to CBS-myoglobin (A-D) or TIP-myoglobin. Analyte concentrations were 1000 nM (green), 500 nM (magenta), 250 nM (orange), 125 nM (red), and 63 nM (blue). Fits are shown to a single-state global model for which the constants are shown in Table 1. F, EDTA dissociation phases for 1000 nM analyte samples moved into EDTA after dissociation phase. Binding normalized to % specific binding to eliminate differences in amplitude, allowing direct comparisons.

<https://doi.org/10.1371/journal.pone.0178648.g001>

Table 2. Kinetic and affinity constants for CPP-adaptor binding to CBS-myoglobin (or TIP-myoglobin).

Constant	TAT-CaM 2.0	TAT-CALML3	SAP-CaM	SAP(E)-CaM	TAT-Troponin
k_{on} ($M^{-1}s^{-1}$)	4900	6100	8300	9400	3700
k_{off} (s^{-1})	ND	1.8×10^{-4}	1.7×10^{-4}	1.3×10^{-4}	ND
K_D (nM)	ND	29.8	20.6	13.3	ND
k_{off} (EDTA) (s^{-1})	0.17	0.07	0.11	0.20	0.018

Kinetic and affinity constants as determined from global fits of sensorgrams shown in Fig 1. ND, not determined.

<https://doi.org/10.1371/journal.pone.0178648.t002>

was not widely distributed throughout the cytoplasm, i.e. the time it took from treatment to image acquisition was longer than penetration and release. Rapid cytoplasmic distribution is consistent with rapid loss of endocytosed Ca^{2+} coincident with acidification of endosomes [23].

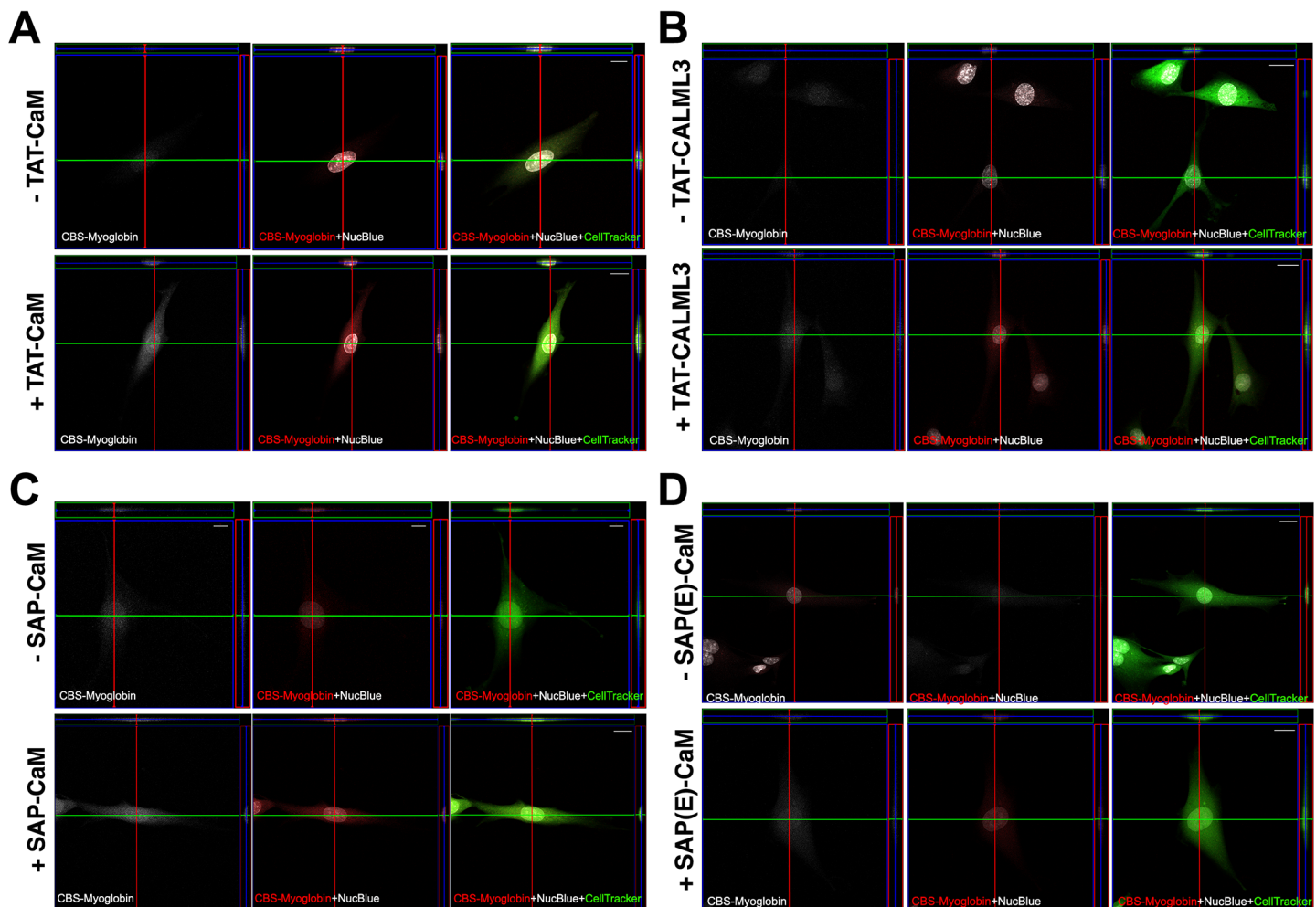


Fig 2. Cell penetration assay for a variety of CPPs and adaptor proteins for delivery of myoglobin to BHK cells. Each panel are images from experiments with different CPP-adaptors: A, TAT-CaM 2.0; B, CALML3; C, SAP-CaM; D, SAP(E)-CaM. BHK cells were treated for 1 h with DyLight 550 fluorescently labeled CBS-myoglobin (rendered as white in left panels, red in center and right panels), in either the absence or presence of CPP-adaptor, washed and imaged live. Center images are optical sections set at a similar depth of the nucleus (NucBlue staining, white, center and right panels), as determined by position within the Z-stack. Orthogonal projections are shown at the right (boxed in red) and top (boxed in green) sides of each panel. Cytoplasmic compartments in live cells were visualized using CellTracker Green CMFDA dye (green in right panels). Comparison of CPP-adaptor-treated versus untreated cells indicates that in all cases, myoglobin was delivered and localized primarily to the cytoplasm. Scale bars in all panels, 20 μm .

<https://doi.org/10.1371/journal.pone.0178648.g002>

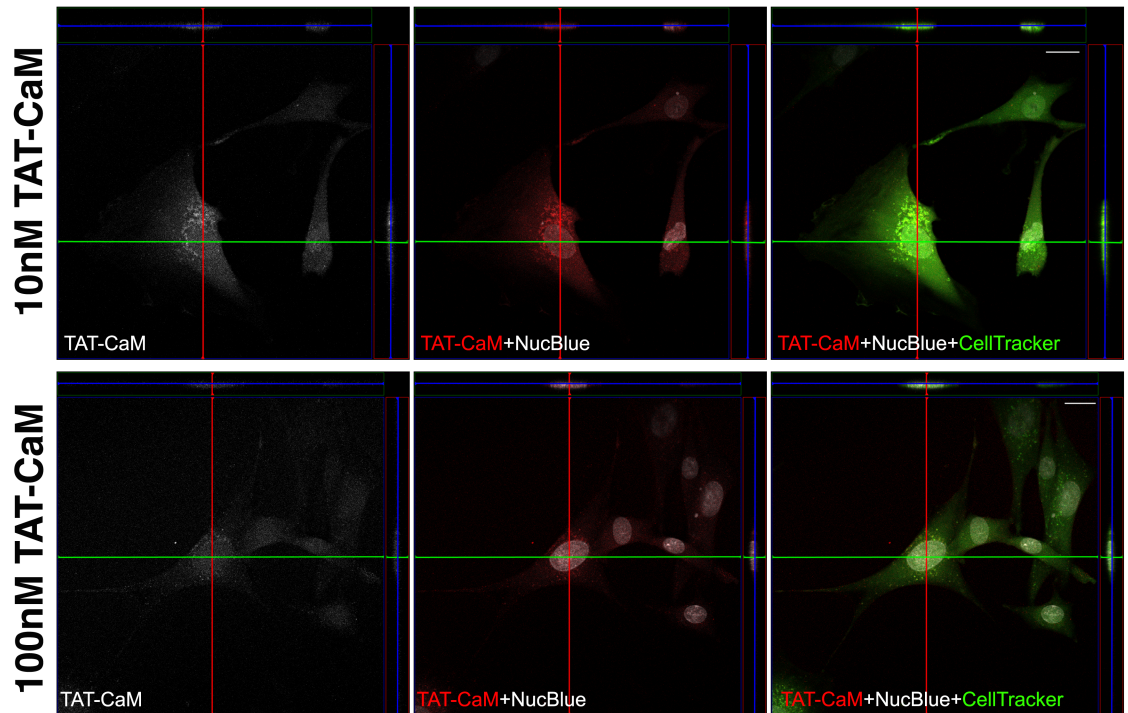


Fig 3. TAT-CaM localization. Cell penetration assay performed with complexes of fluorescently labelled TAT-CaM and unlabeled myoglobin at 10 nM (top) and 100 nM (bottom). Fluorescence rendering is the same as Fig 1 (Dylight fluorescence is white in the left panels and red in the center and right panels).

<https://doi.org/10.1371/journal.pone.0178648.g003>

What of TAT-CaM? Does it get into the cytoplasm or is it trapped in endosomes as other TAT constructs? To address whether our CPP-adaptor is fundamentally the same as other TAT moieties, a penetration experiment was conducted in which TAT-CaM was labelled and CBS-myoglobin was unlabeled (Fig 3A). As expected, TAT-CaM exhibited a punctate distribution

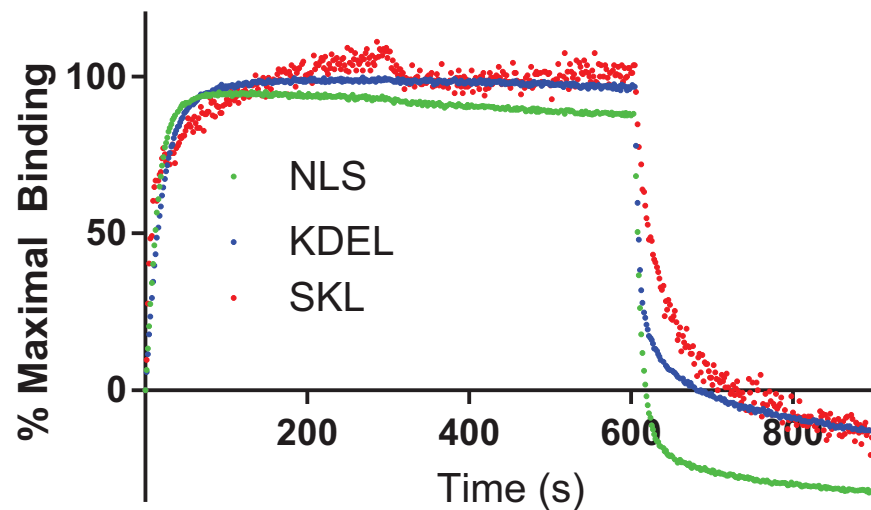


Fig 4. Biolayer interferometry analysis of subcellular localization constructs. TAT-CaM was used as ligand and analytes were CBS-myoglobin-NLS (green), CBS-myoglobin-KDEL (blue), CBS-myoglobin-SKL (red). Phases, analyte concentrations and fits are the same as in Fig 1.

<https://doi.org/10.1371/journal.pone.0178648.g004>

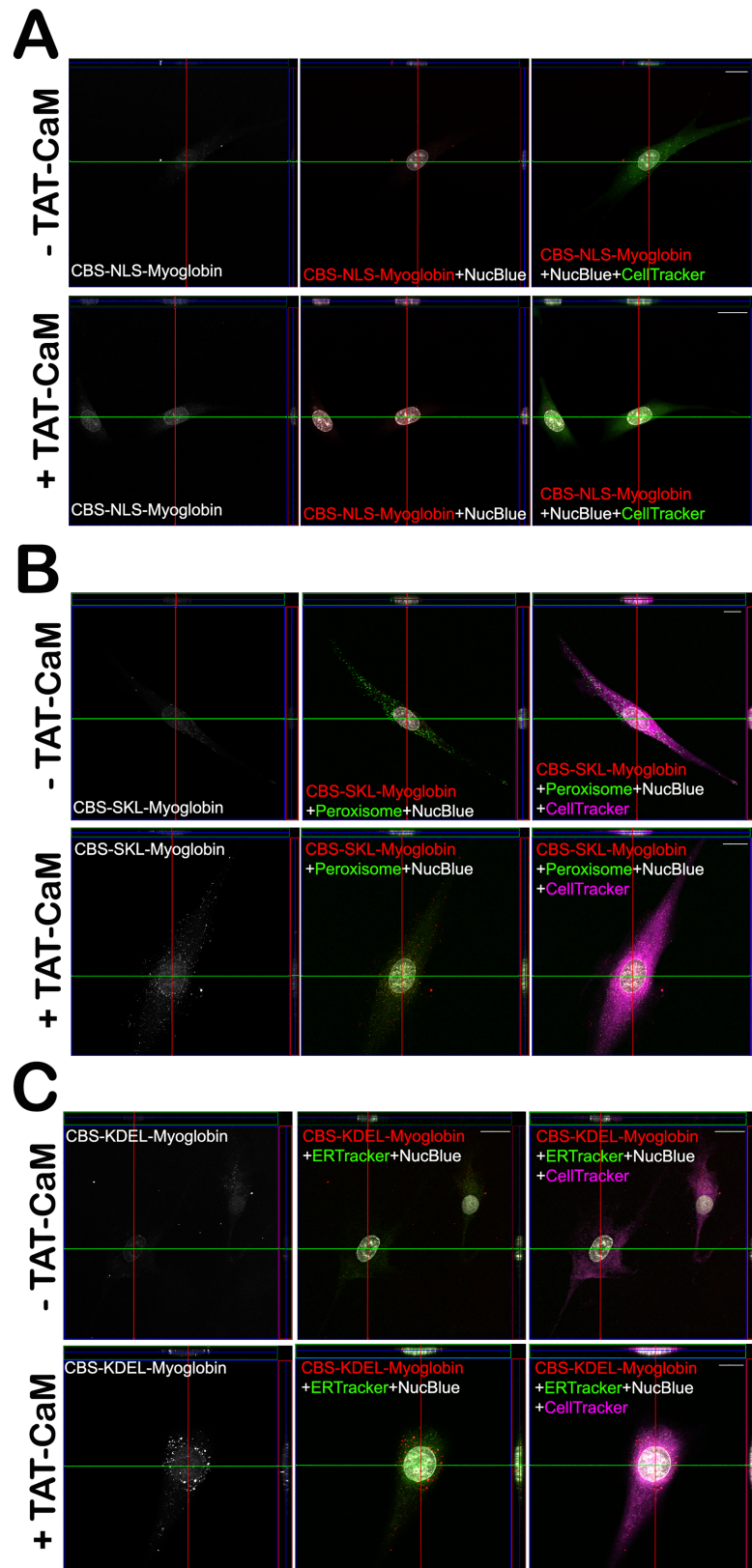


Fig 5. Cell penetration assay for subcellular localization. Each panel are images from a different cargo protein: A, CBS-myo-NLS (nuclear localization signal); B, CBS-myo-SKL (peroxisome signal); C, CBS-myo-

KDEL (endoplasmic reticulum signal). Cells were treated and images are rendered the same as Fig 2 except that for panels B and C, CellTracker (cytoplasmic marker) is purple and either peroxisome (B) or ER (C) markers are rendered in green. Comparison of CPP-adaptor-treated versus untreated cells indicates that in all cases, myoglobin was delivered and localized to the appropriate subcellular compartment. Scale bars in all panels, 20 μ m.

<https://doi.org/10.1371/journal.pone.0178648.g005>

consistent with endosomal localization. To confirm the result, a similar assay was conducted with unlabeled proteins, after which cells were fixed and then exposed to anti-calmodulin and a fluorescently labelled secondary antibody (S1 Fig). The punctate distribution of TAT-CaM was pronounced, leading to the conclusion that indeed, our TAT-CaM remains trapped in the endosomes but releases cargo for subsequent escape to the cytoplasm.

CPP-mediated delivery of cargos to subcellular compartments has long been desired but has similarly been stymied by the endosomal escape problem [11]. Having demonstrated the advantages of our noncovalent linking strategy, we also sought to use recombinant cargos with subcellular localization signals. CBS-myo constructs with C-terminal subcellular localization signals were expressed, purified and analyzed with respect to binding, penetration and localization. Localization signals examined were nuclear (SV40 large T antigen signal, PKKKRKV), peroxisomal (SKL) and endoplasmic reticulum (KDEL)[34]. As expected (Fig 4), all constructs

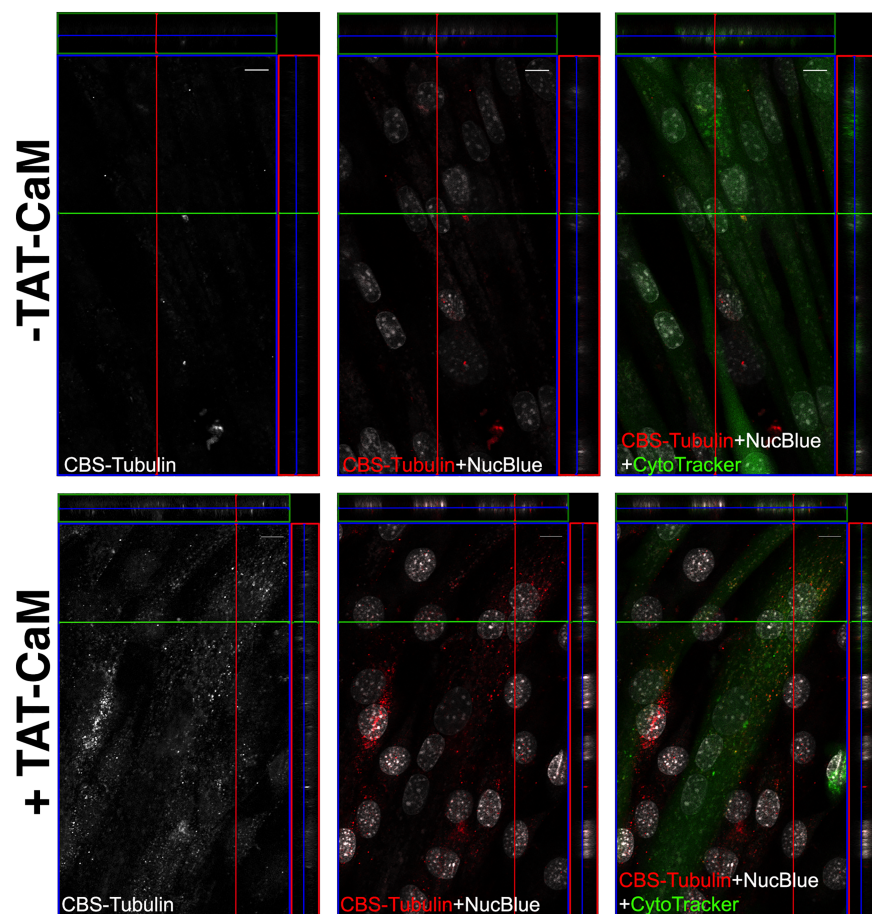


Fig 6. Cell penetration in myotubes. DyLight 550-labelled tubulin was used as cargo for TAT-CaM-mediated delivery to myotubes. Colors are rendered as in Fig 2.

<https://doi.org/10.1371/journal.pone.0178648.g006>

exhibited high affinity, fast-on, slow-off binding to TAT-CaM in the presence of calcium and rapid dissociation in the presence of EDTA. Full characterizations were not done and amplitude was normalized to percent maximal binding because the binding experiments were performed with different ligand preparations. Signal less than zero in the EDTA phase is likely a result of association and EDTA-induced dissociation phases so rapid that a significant amount occurred during transitions of the sensor from baseline to association and from dissociation to EDTA dissociation; the instrument takes a reading every 1.6 seconds; rapid binding or dissociation can cause uncertainty as to where 0 nm shift is.

All localization signals exhibited delivery to intended destinations (Fig 5). Addition of either nuclear localization sequence, KDEL, or SKL tags resulted in delivery of cargo protein to either the nuclei, ER, or the peroxisomes indicated by colocalization with the respective compartment labels. To our knowledge, our CPP-adaptor system is first CPP-mediated delivery method to readily achieve efficient penetration and disparate distribution. That it is relatively simple, utilizing the well-studied TAT sequence, reversible high-affinity binding and consensus localization signals strongly suggest its general utility as a research tool and hint at its promise for therapeutic delivery.

Conventional liposomal transfection protocols require recipient cells to be actively dividing. However, differentiated cell structures, such as cultured mouse myotubes, are notoriously difficult to transfect using nonviral or non-electroporation based methods, as these fully differentiated cells have largely exited the cell cycle [35]. Our protein delivery method can likely overcome this barrier. To address the facility of delivery of cargo to such a cell line, we assayed fused, differentiated C2C12 myotubes for delivery of CBS- α -tubulin. As expected, cargo tubulin was delivered in the presence, but not the absence of TAT-CaM, and its distribution was found throughout the cytoplasm (Fig 6). We are tremendously excited by this finding, as we have successfully delivered a cargo of choice in a safe, non-viral method, to a fully differentiated tissue structure, under largely normal tissue culture conditions.

Supporting information

S1 Fig. Immunohistological confirmation of TAT-CaM localization. BHK cells were treated with TAT-CaM complexed with CBS-Myo (100 nM each) for 15 min. Cells were washed in PBS 3 times and then fixed with 4% PFA and 0.1% Triton-X-100 with rocking at room temperature for 20 min, then blocked with PBS/5% BSA for an hour. The fixed cells were probed overnight at 4°C with a 1:1000 dilution of anti-calmodulin (Thermo Fisher). Localization was observed using a 1:200 dilution Alexa 488-labelled goat anti-rabbit Alexa 488. (PPTX)

Author Contributions

Conceptualization: VMN JLM SJN CAC.

Data curation: VMN DSA ANH SJN JLM.

Formal analysis: JLM SJN VMN ANH DSA.

Funding acquisition: JLM CAC SJN.

Investigation: VMN DSA ANH SJN CAC JLM.

Methodology: VMN SJN JLM.

Project administration: JLM.

Resources: JLM SJN.

Supervision: JLM.

Validation: VMN DSA ANH SJN CAC JLM.

Visualization: VMN SJN JLM DSA ANH.

Writing – original draft: JLM SJN.

Writing – review & editing: VMN DSA ANH SJN CAC JLM.

References

1. Agrawal P, Bhalla S, Usmani SS, Singh S, Chaudhary K, Raghava GPS, et al. CPPsite 2.0: a repository of experimentally validated cell-penetrating peptides. *Nucl Acids Res.* 2016; 44:D1098–D1103. <https://doi.org/10.1093/nar/gkv1266> PMID: 26586798
2. Gautam A, Singh H, Tyagi A, Chaudhary K, Kumar R, Kapoor P, et al. CPPsite: a curated database of cell penetrating peptides. *Database (Oxford).* 2012; 7.
3. Henriques ST, Costa J, Castanho MA. Translocation of beta-galactosidase mediated by the cell-penetrating peptide of pep-1 into lipid vesicles and human HeLa cells is driven by membrane electrostatic potential. *Biochemistry.* 2005; 44(30):10189–98. <https://doi.org/10.1021/bi0502644> PMID: 16042396
4. Presente A, Dowdy SF. PTD/PPP peptide-mediated delivery of siRNAs. *Curr Pharm Design.* 2013; 19:2943–7.
5. Fonseca SB, Pereira MP, Kelley SO. Recent advances in the use of cell-penetrating peptides for medical and biological applications. *Adv Drug Deliv Rev.* 2009; 61:953–64. <https://doi.org/10.1016/j.addr.2009.06.001> PMID: 19538995
6. Sebbage V. Cell-penetrating peptides and their therapeutic applications. *Biosci Horizons.* 2009; 2:64–72.
7. Johnson RM, Harrison SD, Maclean D. Therapeutic applications of cell-penetrating peptides. *Methods Mol Biol* 2011; 683:535–51. https://doi.org/10.1007/978-1-60761-919-2_38 PMID: 21053155
8. Lonn P, Dowdy SF. Cationic PTD/PPP-mediated macromolecular delivery: charging into the cell. *Expert Opin Drug Deliv.* 2015; 26:1–10.
9. Madani F, Lindberg S, Langel U, Futaki S, Graselund A. Mechanisms of cellular uptake of cell-penetrating peptides. *J Biophys.* 2011; 2011:414729. <https://doi.org/10.1155/2011/414729> PMID: 21687343
10. Duchardt F, Fotin-Mleczek M, Schwarz H, Fischer R, Brock R. A comprehensive model for the cellular uptake of cationic cell-penetrating peptides. *Traffic.* 2007; 8(7):848–66. <https://doi.org/10.1111/j.1600-0854.2007.00572.x> PMID: 17587406
11. Kawaguchi Y, Takeuchi T, Kuwata K, Chiba J, Hatanaka Y, Nakase I, et al. Syndecan-4 Is a Receptor for Clathrin-Mediated Endocytosis of Arginine-Rich Cell-Penetrating Peptides. *Bioconjugate Chemistry.* 2016; 27(4):1119–30. <https://doi.org/10.1021/acs.bioconjchem.6b00082> PMID: 27019270
12. Fuchs H, Bachran C, Li T, Heisler I, Dürkop H, Sutherland M. A cleavable molecular adapter reduces side effects and concomitantly enhances efficacy in tumor treatment by targeted toxins in mice. *Journal of Controlled Release.* 2007; 117(3):342–50. <https://doi.org/10.1016/j.jconrel.2006.11.019> PMID: 17207883
13. Erazo-Oliveras A, Najjar K, Dayani L, Wang TY, Johnson GA, Pellois JP. Protein delivery into live cells by incubation with an endosomolytic agent. *Nat Methods.* 2014; 11(8):861–7. <https://doi.org/10.1038/nmeth.2998> PMID: 24930129
14. Xie X, Yang Y, Yang Y, Mei X. Photolabile-caged peptide-conjugated liposomes for siRNA delivery. *J Drug Target.* 2015; 39(9):789–99.
15. Salerno JC, Ngwa VM, Nowak SJ, Chrestensen CA, Healey AN, McMurry JL. Novel cell penetrating peptides effect intracellular delivery and endosomal escape of desired protein cargos. *J Cell Sci.* 2016; 129:893–7. <https://doi.org/10.1242/jcs.182113> PMID: 26801086
16. Vivès E, Brodin P, Lebleu B. A Truncated HIV-1 Tat Protein Basic Domain Rapidly Translocates through the Plasma Membrane and Accumulates in the Cell Nucleus. *Journal of Biological Chemistry.* 1997; 272(25):16010–7. PMID: 9188504
17. Krebs J, Heizmann CW. Calcium-binding proteins and the EF-hand principle. In: Krebs J, Michalak M, editors. *Calcium: A Matter of Life or Death*: Elsevier; 2007.

18. Stratton MM, Chao LH, Schulman H, Kuriyan J. Structural studies on the regulation of Ca^{2+} /calmodulin dependent protein kinase II. *Curr Opin in Struct Biol.* 2013; 23:292–301.
19. Houdusse A, Cohen C. Target sequence recognition by the calmodulin superfamily: implications from light chain binding to the regulatory domain of scallop myosin. *Biochemistry.* 1995; 92:10644–7.
20. Newman E, Spratt DE, Mosher J, Cheyne B, Montgomery HJ, Wilson DL, et al. Differential activation of nitric-oxide synthase isozymes by calmodulin-troponin C chimeras. *J Biol Chem.* 2004; 279(32):33547–57. <https://doi.org/10.1074/jbc.M403892200> PMID: 15138276
21. McMurry JL, Chrestensen CA, Scott IM, Lee EW, Rahn AM, Johansen AM, et al. Rate, affinity and calcium dependence of CaM binding to eNOS and nNOS: effects of phosphorylation. *FEBS J.* 2011; 278(24):4943–54. <https://doi.org/10.1111/j.1742-4658.2011.08395.x> PMID: 22004458
22. Clapham DE. Calcium signaling. *Cell.* 2007; 131(6):1047–58. <https://doi.org/10.1016/j.cell.2007.11.028> PMID: 18083096
23. Gerasimenko JV, Tepikin AV, Petersen OH, Gerasimenko OV. Calcium uptake via endocytosis with rapid release from acidifying endosomes. *Current Biology.* 1998; 8(24):1335–8. PMID: 9843688
24. Fernandez-Carneado J, Kogan MJ, Pujals S, Giralt E. Amphipathic peptides and drug delivery. *Biopolymers.* 2004; 76(2):196–203. <https://doi.org/10.1002/bip.10585> PMID: 15054899
25. Martin I, Teixido M, Giralt E. Design, synthesis and characterization of a new anionic cell-penetrating peptides: SAP(E). *ChemBiochem.* 2011; 12(6):896–903. <https://doi.org/10.1002/cbic.201000679> PMID: 21365733
26. Rhyner JA, Koller M, Durussel-Gerber I, Cox JA, Strehler EE. Characterization of the human calmodulin-like protein expressed in *Escherichia coli*. *Biochemistry.* 1992; 31(51):12826–32. PMID: 1334432
27. Li MX, Saude EJ, Wang X, Pearlston JR, Smillie LB, Sykes BD. Kinetic studies of calcium and cardiac troponin I peptide binding to human cardiac troponin C using NMR spectroscopy. *Eur Biophys J.* 2002; 31:245–56. <https://doi.org/10.1007/s00249-002-0227-1> PMID: 12122471
28. Cerrato CP, Künnapuu K, Langel Ü. Cell-penetrating peptides with intracellular organelle targeting. *Expert Opinion on Drug Delivery.* 2017; 14(2):245–55. <https://doi.org/10.1080/17425247.2016.1213237> PMID: 27426871
29. Nowak SJ, Nahirney PC, Hadjantonakis A-K, Baylies MK. Nap1-mediated actin remodeling is essential for mammalian myoblast function. *J Cell Sci.* 2009; 122:3282–93. <https://doi.org/10.1242/jcs.047597> PMID: 19706686
30. McMurry JL, Minamino T, Furukawa Y, Francis JW, Hill SA, Helms KA, et al. Weak interactions between *Salmonella enterica* FlhB and other flagellar export apparatus proteins govern type III secretion dynamics. *PLOS One.* 2015; 10(8):e0134884. <https://doi.org/10.1371/journal.pone.0134884> PMID: 26244937
31. Dolman NJ, Kilgore JA, Davidson MW. A review of reagents for fluorescence microscopy of cellular compartments and structures, part I: BacMcm labeling and reagents for vesicular structures. *Curr Protoc Cytom.* 2013; 12:12.30.
32. Tan R-Y, Mabuchi Y, Grabarek Z. Blocking the Ca^{2+} -induced conformational transitions in calmodulin with disulfide bonds. *J Biol Chem.* 1996; 271(7479–7483). PMID: 8631777
33. Persechini A, Moncrief ND, Kretsinger RH. The EF-hand family of calcium-modulated proteins. *Trends Neurosci.* 1989; 12(11):462–7. PMID: 2479149
34. Imai K, Nakai K. Prediction of subcellular locations of proteins: Where to proceed? *Proteomics.* 2010; 10:3970–83. <https://doi.org/10.1002/pmic.201000274> PMID: 21080490
35. Balcı B, Dinçer P. Efficient transfection of mouse-derived C2C12 myoblasts using a matrigel basement membrane matrix. *Biotechnology Journal.* 2009; 4(7):1042–5. <https://doi.org/10.1002/biot.200800269> PMID: 19360711